

DIAGNOSTICS AND MODELING OF HIGH PRESSURE STREAMER INDUCED DISCHARGES

E.Marode, P.Dessantes, N.Deschamps, C.Deniset
Laboratoire de Physique des Gaz et des Plasmas, EDEE, SUPELEC, 91192 Gif-Cedex

1. Introduction

Different types of non-thermal plasmas can be generated by the so-called streamer discharge. They all belong to a class of discharges presenting filamentary structures. The term “streamer” refers to the very tiny ionization wave, based on electron avalanches sustained by a high, and confined, space-charge field. The wave propagates rapidly, at some 10^7 cm/s, and leaves, behind it, a filamentary plasma. At this stage, the produced filamentary plasma is in a non-thermal state, with an electron temperature much larger than that of the gas or the ions. The “streamer” is the smallest, but the leading part of a filamentary discharge during its build up, and due to that, is sometimes called improperly “streamer head”. For gaps in the centimetric range, the streamer can cross the gap, and set a conductive filamentary plasma between the two electrodes¹. In view of keeping the non-thermal state of the filamentary plasma, the transition to spark must be avoided. One way is to use a highly stressed electrode, with a small radius. In such case, no spark occur within a certain potential range. If the potential is large and leads normally to a spark, then a control of the current growth can be applied with an appropriate external circuit. Another way is to use a dielectric material set between the electrodes. In such case an alternating applied potential must be used to allow a permanent plasma maintenance. The so-called DBD technique (dielectric barrier discharge), based on such arrangement, develops extended high pressure plasmas made of sets of filamentary discharges simultaneously mixed with homogeneous glow discharge regime. The formation of these filament has been shown to be similar to the streamer filament formation². Thus, a great variety of high pressure plasma are based on streamer build-up. To study these filamentary plasma structures, one approach is to isolate one filamentary discharge by using a positive point-to-plane gap, near atmospheric pressures, and activating it by positive, continuous or pulsed, applied potential. The starting streamer position, in such manner, is well defined near the positive point, and even the filamentary plasma is situated near the gap axis for continuous applied potential, and thus the plasma growth and properties can be better grasped.

A great variety of diagnostic has been applied to gain information on basic parameter governing high pressure non-thermal filamentary plasmas (and namely streamer induced filamentary discharges). Apart from electrical diagnostics, gas discharge, in contrast with solid state physics, can greatly benefit from all optical techniques owing to its “transparent” state. Emission and absorption spectroscopy, as well as LIF³ or CARS (talk are given during this meeting on these two techniques) are among such specific possibilities. The figures gained from these diagnostic measurements has generally no meaning by itself. They must be worked out, by means of calibrated former results, and/or by using them as input in high pressure plasma modeling.

Mixing experimental and modeling approach is necessary for reaching relevant physical knowledge of the high pressure filamentary discharges processes. It will be namely shown that diffusion, and thermal space and time distribution, must fully be taken into account.

2. Diagnostics on streamer induced discharges

2.1. Electrical and light emission features

A high positive voltage, dc or pulsed, is applied to a point to plane gap (figure 1). The mean value of the discharge current is measured by a micro-ammeter in series with the gap. The current however is composed of series of discharge pulses superimposed on a dc current. The discharge current pulses are measured by recording the voltage appearing on a resistor r with a high-speed oscilloscope. The difference between the mean current (in red) and the dc component (in green) corresponds to the mean value of the current when the current pulses are integrated in time. The pulse frequencies are indicated below. The current pulses, named “streamer” pulses, appear like vertical repetitive narrow blue pulses at low sweeping rate. They are associated with very small potential falls (in blue). The streamer pulse detail appears below. For larger applied potential (in red), the streamer pulse is followed by the spark

pulse, which now, is associated with a complete transient potential fall. The current detail in that case, figure 1, reveals the general current shape, with a current depression separating the streamer pulse from the spark pulse. Notice the much larger streamer pulse which triggers the spark.

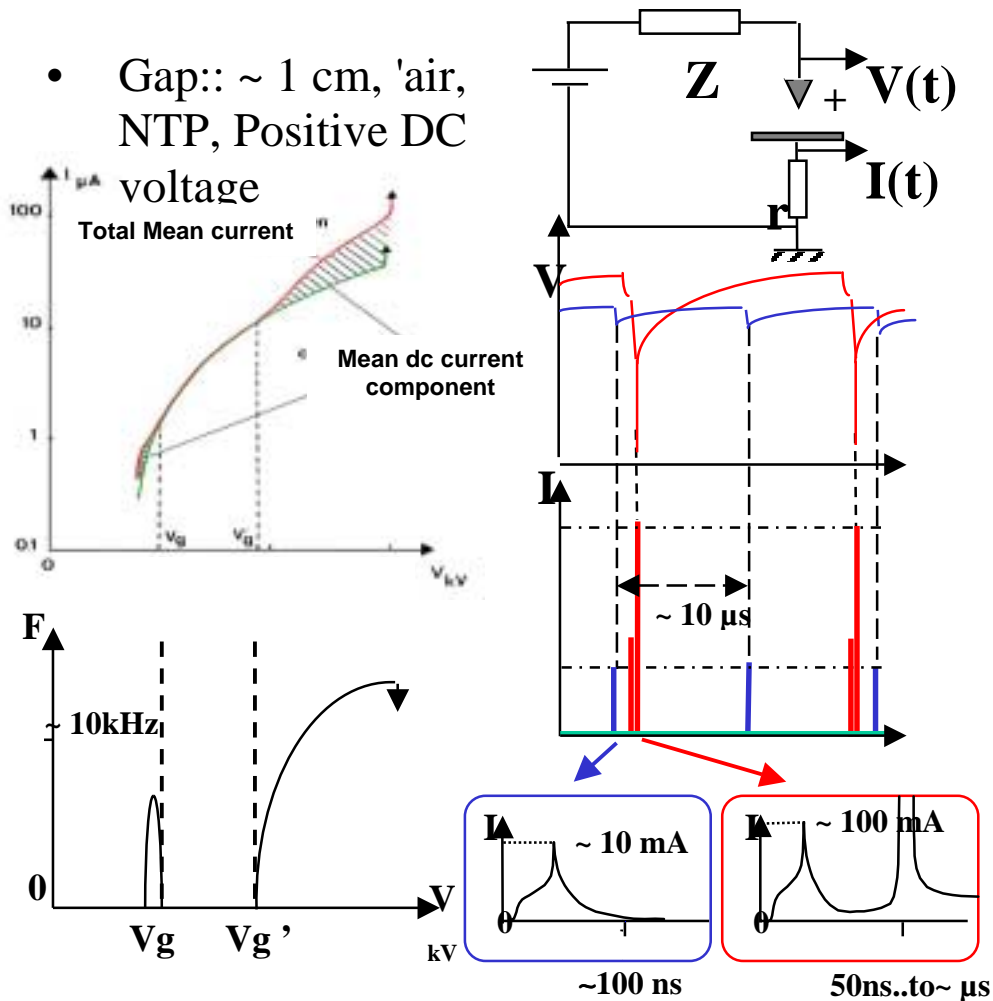


figure 1 Electrical feature of streamer induced discharges

One of the earlier diagnostics, is the use of streak camera to follow the streamer light emission behaviour. Figure 2 summarizes earlier findings. A streak camera of the streamer induced transition to spark under DC high voltage, gives the spatial distribution of the filamentary discharge (the discharge lies along the gap axis) at each time. On figure 2 the associated current pulse is given, similar to that given in figure 1. The streamer propagation is clearly seen. It is associated with the first part of the streamer pulse. As soon as the streamer reaches the plane electrode, the current rises strongly, indicated the moment when the plasma bridge between the electrodes is created. The shape, and reason of that shape has been already fully described elsewhere⁴. Let us just recall briefly the main processes. The decrease of the streamer pulse is due to electron attachment along the filamentary plasma. During the current pulse, the cylindrical plasma core is slightly heated, inducing a rise of the gas temperature and an associated pressure rise. The resulting pressure gradient which sets with the surrounding of the discharge, leads to a hydrodynamic expansion which induce a decrease of neutral density within the discharge. The ratio, field to density E/N , increases until the electron ionization rate begin to exceed the attachment rate. In such case the current increases again, and leads to the spark formation. The hollow part of the current is due to the hydrodynamic delay. If the streamer pulse is smaller the delay may be microseconds, while if it increases no more hollow current part can be observed.

Spectroscopic diagnostic has been applied to estimate the electron temperature for the several discharge part. Notice the difference between that estimated within the streamer (10-30 eV), and that within the filamentary plasma channel (1.4 eV). These figures are extracted from the intensity ratio between the second positive group of nitrogen N_2 and the first negative group of the nitrogen ion N_2^+ .

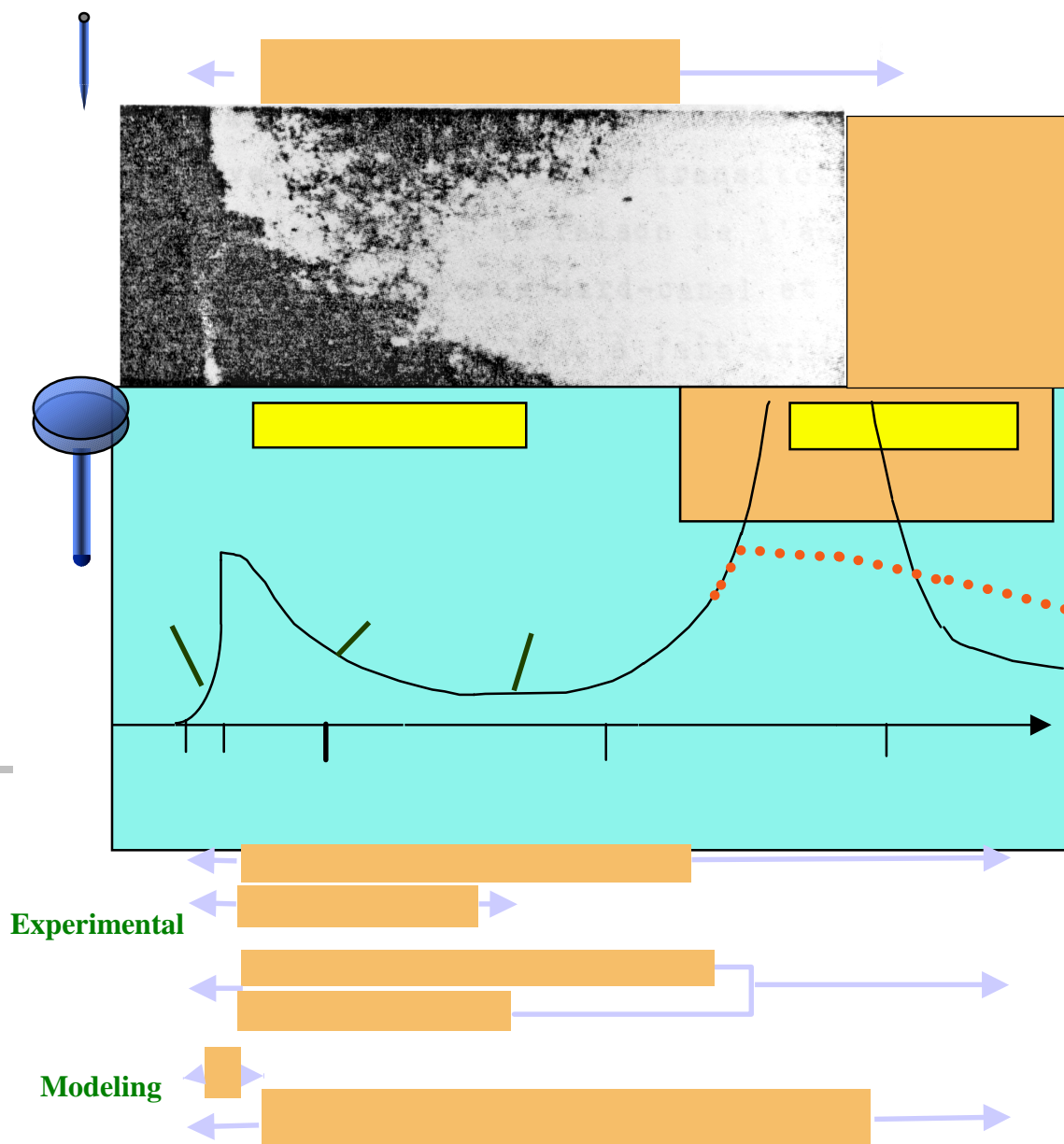


figure 2 Current pulse and time resolved streak camera image of the streamer induced transition to spark. Various technology research are focused on the indicated segment.

2.2. Emission spectroscopy: Time resolved temperature measurements

The discharge filament is focused perpendicularly to the slit of a HR640 Jobin Yvon monochromator with a magnification of 1. From the positive point the self repetitive streamer discharges are launched with a periode in the range of 60 to 120 μ s. By means of oscilloscopic averaging, the intensity spectrum between 335 and 337 nm is recorded with a step of 0.05 nm and a spectral resolution of 0.1 nm. A specific narrow region of the discharge axis is viewed (figure 3).

The photomultiplier signal for a given wavelength shows a first peak corresponding to the streamer passage, and second peak corresponding to the light emitted by the filamentary plasma (figure 4). Using a temporal window gate (from t to $t+dt$ with $dt \sim 5$ ns) the signal delivered by the photomultiplier during this window time is stored for each wave length, thus obtaining a whole rotational spectrum of a band of the second positive nitrogen system (337 nm).

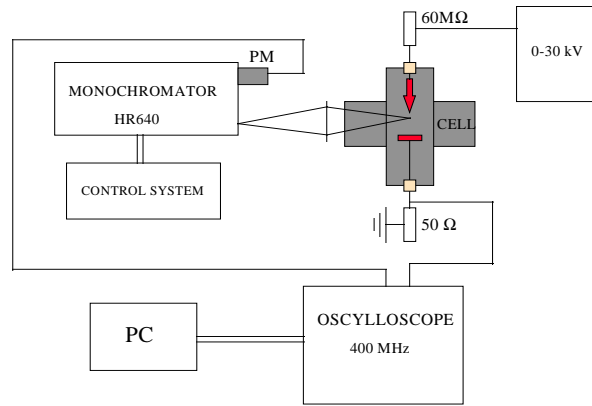


figure 3. The arrangements for studying time resolved discharge spectroscopy

Intensity of given wave length (a.u)

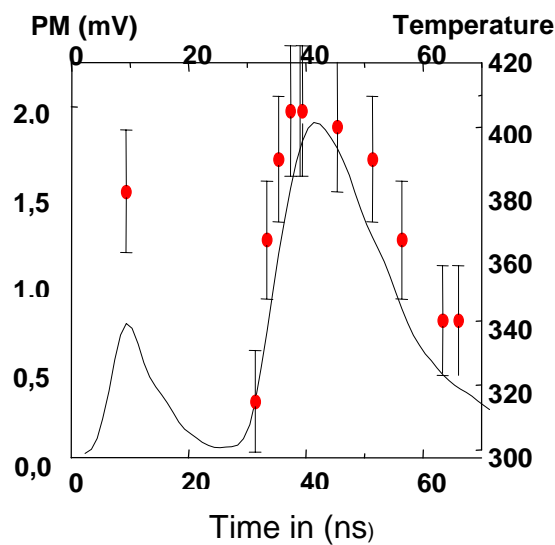
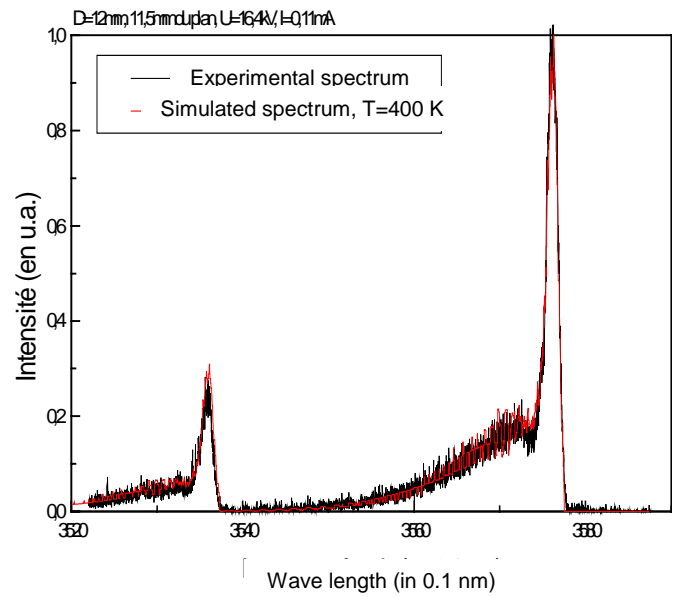
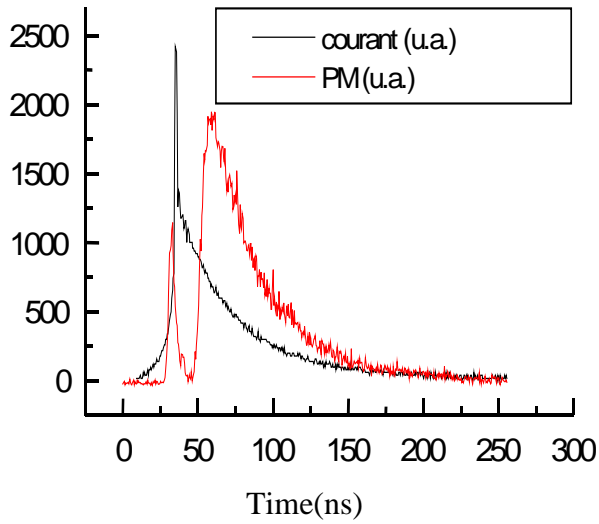


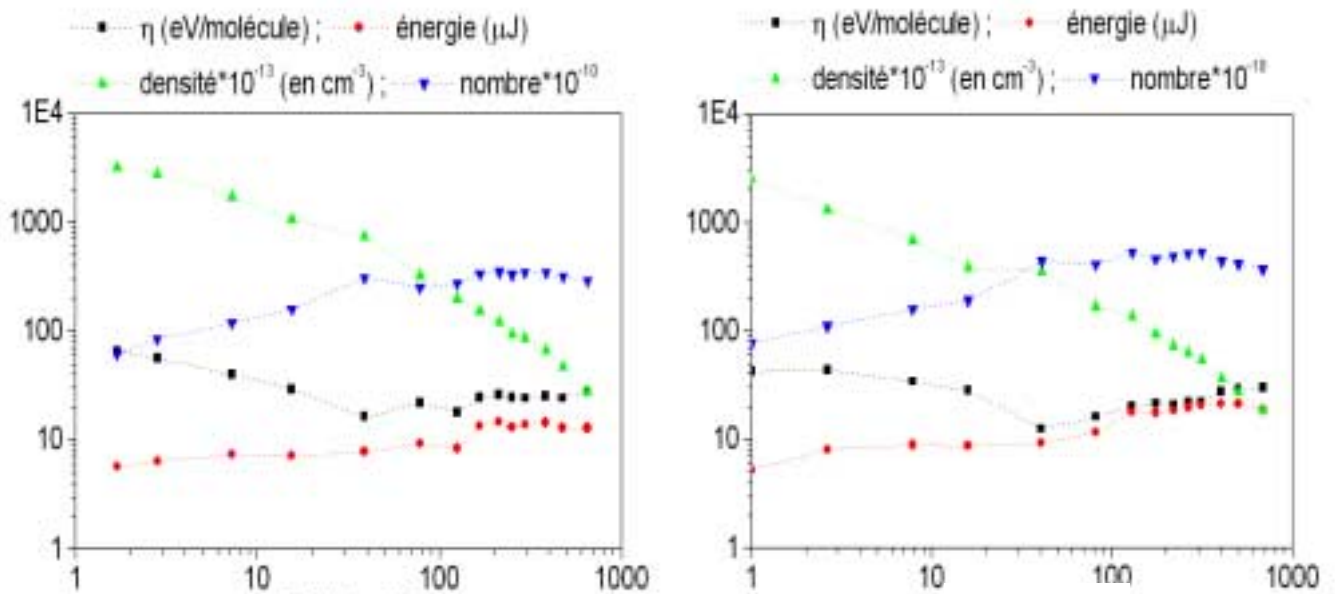
figure 4 Example of recorded pulse and comparison with calculated spectrum. Results of the measurements.

The use of a photomultiplier instead of an OMA allows to have a much better signal to noise ratio. The temperature

is then deduced by fitting this spectrum with a calculated synthetic spectrum based on the same apparatus function (an example of fitting is given). With these sets of data, we are able to follow the variation of the rotational distribution of the band during the development of the discharge. As seen, the time resolved rotational temperature shows rapid changes in time (red points) and a photomultiplier curve is given to situate at which discharge sequence corresponds the data. It is taken 9 mm from the negative plane at 10.8 kV with a repetition rate of 70 μ s and an energy per pulse of 14 μ J. The temperature T_r , is 380 K for the streamer while, after a pronounced dip, the temperature increases again until reaching values of order of 400 K. It is remarkable that the temperature decreases to 315 K in a time as small as 20 ns. Still remarkable is the rapide decrease from 400 to 360K after the maximum. Those quick temperature change cannot be explained by simple thermal conductivity, as will be seen later on.

2.3. Absorption spectroscopy: Measurements of ozone production by streamers as function of flow rates

Various absorption spectroscopy can be used to identify the chemical activity resulting from high pressure discharges. One of the most used is the FTIR, fourier transform infra-red technique. Another technique is the spectrophotometer technique, which uses absorption bands in U.V. region. It is widely used for mesuring the ozone produced by means of discharges. One of the most important ozone UV absorption band is the so-called Hartley band which range from 200 to 300 nm, The absorption cross section of the wavelength $\lambda=253.7$ nm by the ozone is $\sigma_\lambda=10^{-17}$ cm² for. From measure of the decrease of the intensity of a UV beam, crossing a gas flow after its exposition to repetitive streamers, the streamer produced ozone quantity can be derived. The ozone production has been recorded using either a mercury lamp or a deuterium lamp as light source. The discharge is situated at the input of a quartz tube and the flow rate has been changed to study the influence of the gas speed crossing the discharge.



U = 7 kV; f = 30 kHz

U = 6,5 kV; f = 9,3 kHz

figure 5 Ozone produced by streamers as a function of the gas flow through the discharge

When the gas flow increases (figure 5) the recorded ozone density in green decreases as seen for the DC voltage case. This is quite clear, since the produced ozone is diluted into a more and more large volume. However the number of produced ozone molecule per streamer discharge in blue increases, while the energy spent per discharge in red increases too. From these two measurements, the energy cost per ozone molecule, in black, is derived, and a minimum cost at some 100 l/h, which corresponds in our device to about 1m/s, is observed. The same observation is done for pulsed voltage condition. If one observes the discharge region when this minimum is reached, the discharge, instead of crossing steadily the same spatial trajectory, begin to fluctuate a lot. This observation will be used in modeling.

3. Modeling streamers and its filamentary plasma

3.1. Temperature and diffusion

The spark formation, as well as the non-thermal chemistry strongly depends on temperature. The temperature has several different actions. It affects the gas density N (through $p=NkT$) and thus the E/N ratio. Since the electron temperature T_e is a function of E/N , it is an indirect function of T . Thus through T , inelastic electron collisions may be fostered. Also if N changes, the three body heavy species reactions can be affected. On the other hand, the heavy species reaction constants are a direct function of T . Thus, the effect of temperature changes, which we have shown to be observed experimentally, should deserve specific attention. It is the reason why models, taking temperature and neutral density time variation into account, has been developed.

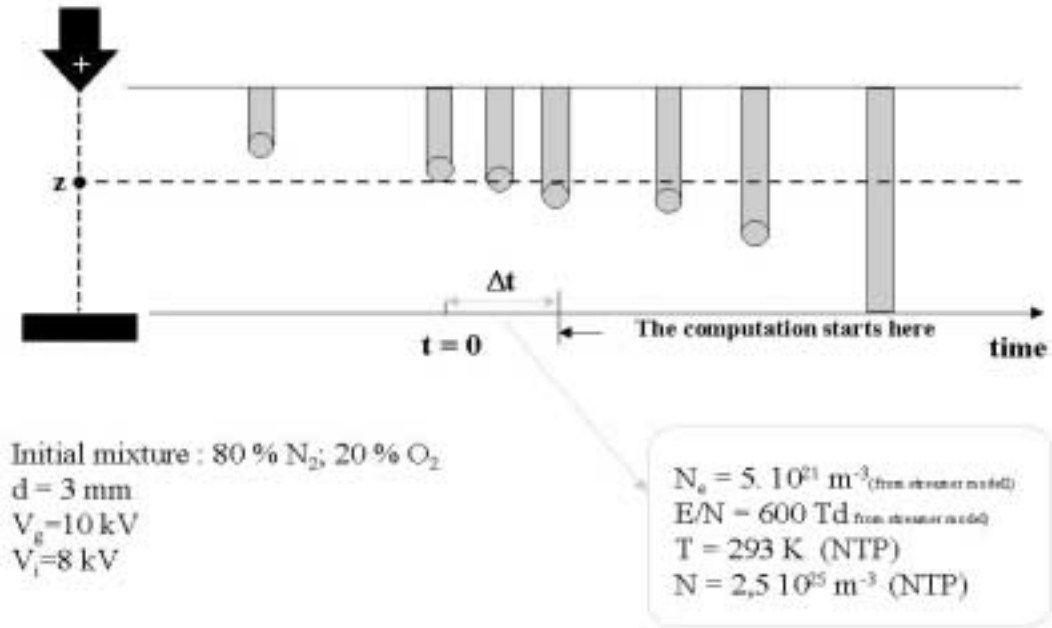


figure 6 Schematic streak sketch illustrating the way the modeling applies.

Using a discharge radius of 20 micrometers (see section 3.2), two modeling approaches has been developed. A simplified one which assumes that the plasma is homogeneous across the section of the discharge cylinder, and a more complete one taking the radial description fully into account⁵. We recall here the set of equations of the full model only, and give some result obtained with the simplified version. As seen on figure 6, the model describe the radial distribution of the discharge parameter around a position z , along the discharge axis. The figure shows that at time $t=0$, the streamer begin to cross position z . After a time Δt , the cylindrical filamentary plasma sets around z . The computation of the set of equations which follows starts at that time Δt . Obviously, the streamer has already left some electrons and some chemical dissociation in the gas. These changes are computed separately by another (2D) modeling. Since a complete two dimensional model of the hydrodynamic approach is for the moment not reachable, the axial field E_z is simply obtained by dividing the gap potential by it length. The time evolution of the current is then given by : $I_d(t) = \int eE_z (N_+ \mu_+ - N_e \mu_e - N_n \mu_n) * 2\pi r dr$, where the N are the various charged species, computed from the following hydrodynamic equations, and the μ the mobilities of the different species. With α , η the ionization and attachment coefficients, the r_{xx} the recombination coefficients, the continuity: equations are:

$$\frac{\partial N^S}{\partial t} + \frac{1}{r} \frac{\partial}{\partial r} (r N^S V^S) = \sum_j \pm k_j(T) N_j N_m N_n + \sum_e \pm k_e(T_e) N_j N_m$$

$$\frac{\partial N_e}{\partial t} + \frac{1}{r} \frac{\partial}{\partial r} (r V_e N_e) = (\alpha - \eta) \mu_e E_z N_e - r_{ei} \left(\frac{T_0}{T} \right)^{2,5} N_e N_+$$

$$\frac{\partial N_+}{\partial t} + \frac{1}{r} \frac{\partial}{\partial r} (r V_+ N_+) = \alpha \mu_e E_z N_e - r_{ii} \left(\frac{T_0}{T} \right)^{2,5} N_- N_+ - r_{ei} \left(\frac{T_0}{T} \right)^{2,5} N_e N_+$$

$$\frac{\partial N_-}{\partial t} + \frac{1}{r} \frac{\partial}{\partial r} (r V_- N_-) = \eta \mu_e E_z N_e - r_{ii} \left(\frac{T_0}{T} \right)^{2,5} N_- N_+$$

Here N^s are the various neutral species, the index s taking several values according to the specific neutral species, atoms, molecules, excited states, radicals, etc...With the mass m , k the Boltzmann constant, the moment transfert equations are:

$$\frac{\partial(N^s V^s)}{\partial t} + \frac{1}{r} \frac{\partial}{\partial r} (r N^s V^s V^s) + \frac{k}{m^s} \frac{\partial}{\partial r} (N^s T) = \frac{1}{m^s} \sum \frac{kT}{g D^s} N^s (V^s - V^g)$$

$$\frac{\partial}{\partial t} (N_+ V_+) + \frac{1}{r} \frac{\partial}{\partial r} (r N_+ V_+^2) + \frac{k}{m^s} \frac{\partial}{\partial r} (N_+ T) - \frac{q E_r}{m^s} N_+ = - \frac{1}{m^s} \sum \frac{kT}{g D_+} N_+ (V_+ - V^g)$$

$$V_e = V_- = V_+$$

$$\frac{1}{r} \frac{\partial}{\partial r} (r E_r) = \frac{\rho}{\epsilon_0}$$

Where the radial component of the electrical field E_r is given by the poisson equation. The f , being the various amounts of energy transfer, an energy balance equation is written:

$$\frac{5}{2} \frac{\partial}{\partial t} (NkT) + \frac{5}{2} \frac{1}{r} \frac{\partial}{\partial r} (r kT \sum N^g V^g) + \frac{kT}{r} \sum N^g \frac{\partial}{\partial r} (r V^g) - \frac{\lambda}{r} \frac{\partial}{\partial r} (r \frac{\partial T}{\partial r}) = S_2$$

$$S_2 = (f_e j_e + f_- j_- + f_+ j_+) E_z - \sum \frac{kT^s}{g D^s} N^s (V^s - V^g) V^g \quad \text{et} \quad Q = -\lambda \frac{\partial T}{\partial r}$$

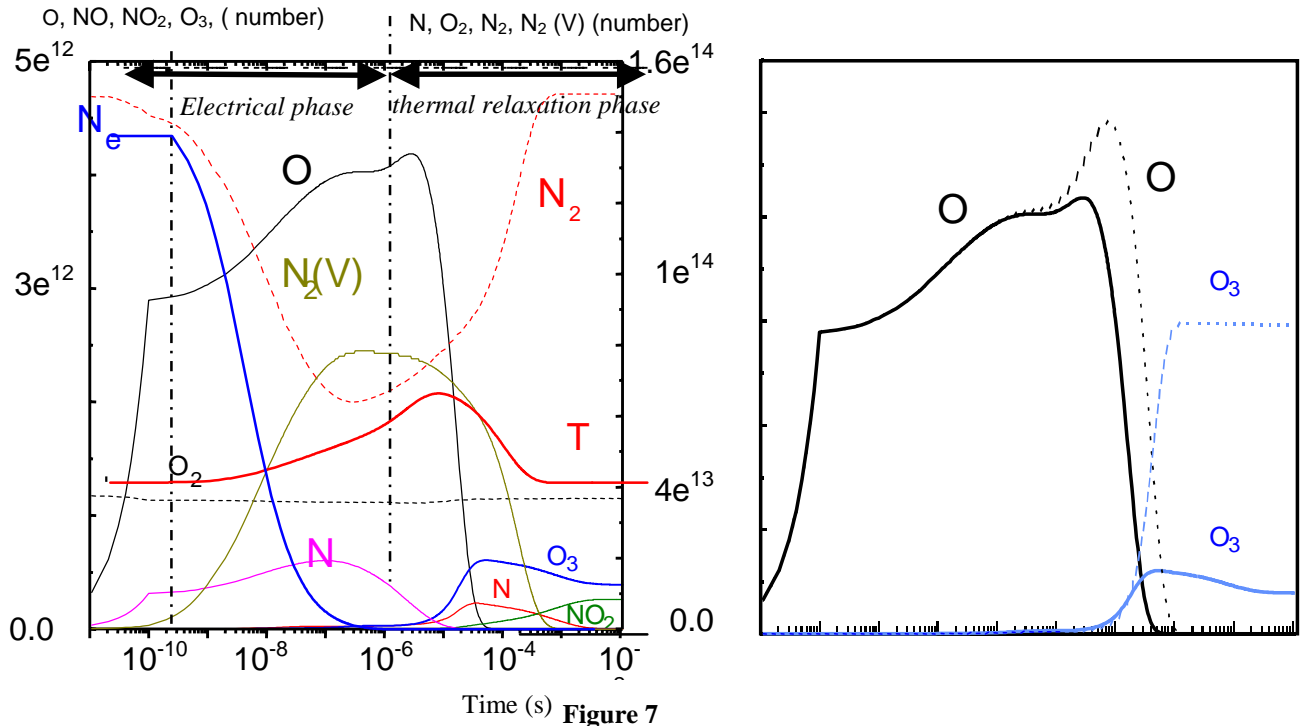
This set of equations has been solved for air at NTP, with the following initial values: $r_0=2 \cdot 10^{-5} \mu\text{m}$, $I_d(t=0)=0.3\text{A}$, $V_g=9.e3$, $d=3.10^{-3}\text{m}$, $f_e=0,5\%$, $f_-=f_+=1$, $r_{ei}=10^{-14}\text{m}^3\text{s}^{-1}$, $r_{ii}=210^{-12}\text{m}^3\text{s}^{-1}$, $\lambda=2.710^{-2}\text{Jdeg}^{-1}\text{m}^{-1}\text{s}^{-1}$. The N_s corresponds successively to the following list.

$$N_s = \{O, N, NO, NO_2, N_2O, NO_3, N_2O_5, O_3, O_2, N_2, N_2(v)\}$$

the reaction constants are taken from [6]. 70 reactions has applied in this case.

As said, the simplified model did not take the radial profile into account. Let us give some results obtained with it, in view of showing what kind of contribution is gained with the full model.

The simplified model clearly show that the electrical phase, i.e., the time during which the transient streamer discharge exist, last only some 10^7 ns while the chemical phase, associated with the thermal relaxation phase is much longer and enter the 10 ms range (and even more). During the electrical phase, atoms are produced by dissociation, and N_2 is vibrationally excited. The electron density N_e decreases due to attachment. N_2 is largely converted into $N_2(v)$, vibrationally excited. During the next phase, the temperature rises. The oxygen is converted partly into ozone O_3 , NO , and NO_2 or reduced back to O_2 .



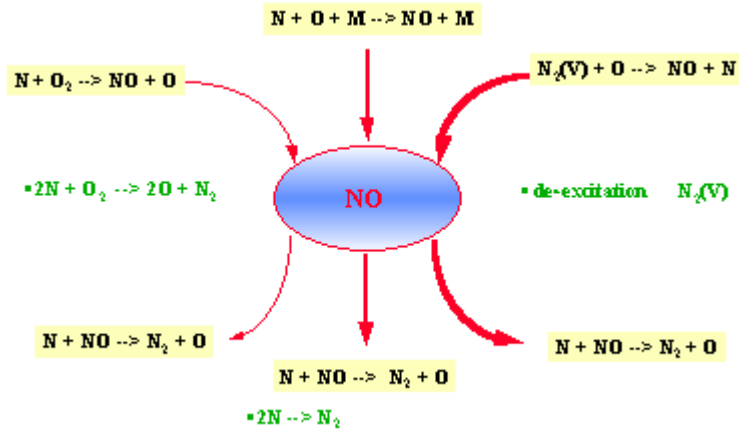


Figure 8. N towards O , a reaction scheme

The ozone production in air compared to that in oxygen is much larger than that which can be guest from the proportion of oxygen into N_2 ⁷. It can be explained as follow. Based on computer analysis, the temperature bump shown at the beginning of the chemical phase induces the reaction scheme sketched above. The NO formation rate is exactly equal to the NO destruction rate. Thus, there is no formation of NO, but NO play the role of a catalyst, which induces the production of two atomic O for two atomic N, increasing the rate of O_3 formation. This process increases with temperature but enter in concurrence with the thermal destruction of ozone (as seen on the left of the following sketch) so that finally, as its stands, the ozone production decreases. However, using a simplified way to take diffusion of species outside the discharge into account, the dotted blue curves for atomic oxygen and ozone

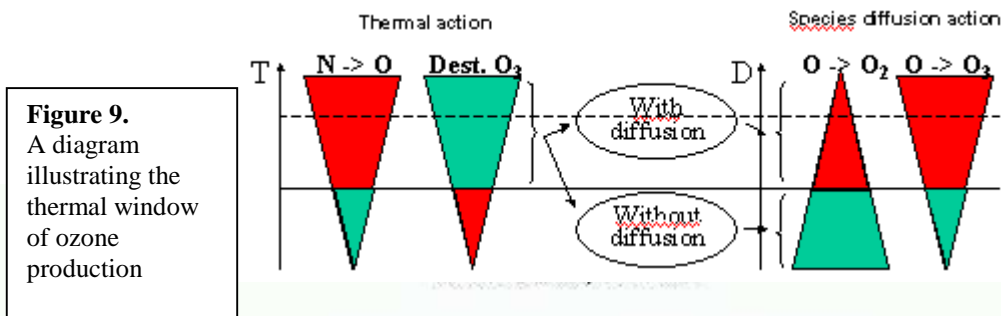


Figure 9. A diagram illustrating the thermal window of ozone production

$d=6mm$ $Rd=20e-6m$ $Z_{prot}=10$ Mohms $i(0)=33mA$
 $V_g=8kV$ $V_c=7.1kV$ $p=1.013e5$ pas $T0=293$

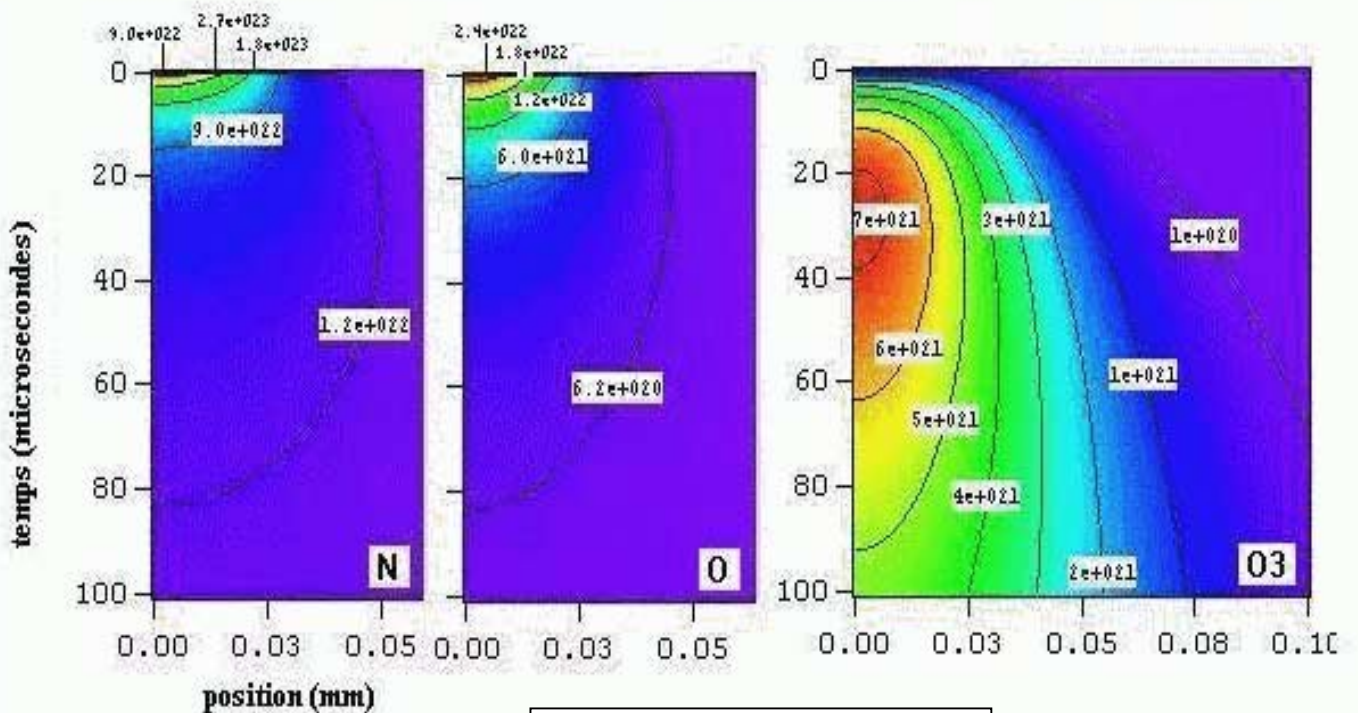


Figure 10. Showing ozone diffusion and time delay of formation

Above figure., which shows some species production as a fonction of time and radial position. Since the discharge radius is 20 micrometers, it is seen that after the early atomic formations, the later ozone formation region diffuses out of the discharge core, and enter a cooler gas section.

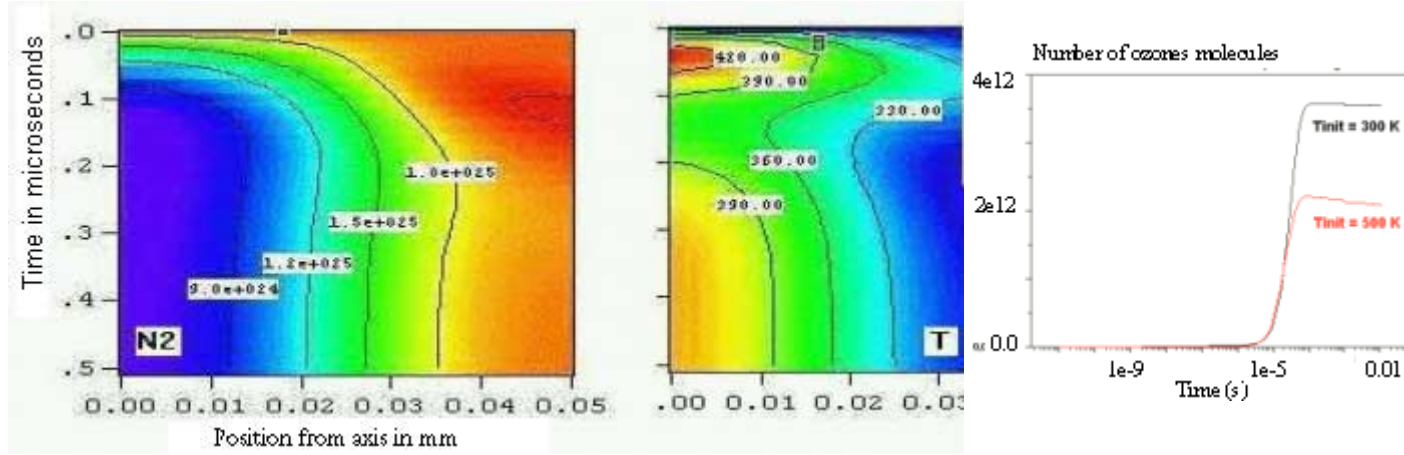


Figure 11 Gas density and temperature spatio-temporal distribution, and effect of initial temperature

In the simplified model the temperature bump is due to vibrational deexcitation. In the full model, vibrational has not been taken into account for the moment. However, the lines of iso-temperature, show that rapid time variation of the temperature associated with the neutral nitrogen gas densities are computed (fig 11). It shows that rapid temperature variations are due to adiabatic expansion cooling or compression heating and not to thermal conductivity cooling.

Blowing on the discharge, disconnect each discharge from the preceding one. It means that they do not follow a “preheated” channel (500k) from previous discharges. Each discharge appears in a cooler fresh gas. Last figure shows the gain in ozone production when, due to blowing, the initial gas temperature is lower.

3.2. The question of the discharge radius

Some year ago, we tried to measure the stark broadening of the hydrogen H_β line, adding hydrogen in tiny proportion to oxygen, and to measure the electron density in a streamer induced filamentary discharge. We actually found out that, due to the space charge field, the measure gives the electron current density rather than the electron density. Dividing the total current by the current density an estimate of the discharge radius gave 20 micrometers⁸. This is the reason for taking such a value. Several bi-dimensional streamer models has been published⁹. Generally they predict a larger radius, at least 70 micrometers. Temperature rise, diffusion and three body reactions rates, depends however strongly, on the size of the filament cross section. There is thus a question concerning why these streamer models do not agree with the experimental estimation. One possible approach is the following. A bi-dimensional treatment of the streamer propagation has been developed in the frame of the previous modeling technique. Let us just recall one of the electron continuity equation treated (see ref 7, Djermoune et al):

$$\frac{\partial n_e}{\partial t} + \frac{\partial}{\partial x} \left(n_e w_{ex} - D_{ex} \frac{\partial n_e}{\partial x} \right) + \frac{1}{r} \frac{\partial}{\partial r} \left[r \left(n_e w_{er} - D_{er} \frac{\partial n_e}{\partial r} \right) \right] = (\alpha - \eta) |V_e| n_e + S_{ph}$$

There is an equation for the positive ions, and negatives ions and excited species n^* as well, and the poisson equation. A new approach has been recently proposed¹⁰. The term S_{ph} is the photo-ionization term, which depends on the de-excitation of the excited species n^* . The term S_{ph} is the rate of photo-electrons produced by absorption of the photon flux $c \varphi_0$, where c is the light speed, and φ_0 the isotropic part of the photon density, while Ψ is the photon angular distribution function. μ is the absorption coefficient, and Γ the probability that an absorbed photon leads to a photo-electron.

$$S_{ph} = \Gamma \mu c \varphi_0(\vec{r}, t)$$

$$\varphi_0(\vec{r}, t) = \int_0^{4\pi} \psi_\nu(\vec{r}, \vec{u}, t) d\vec{u}$$

For each direction \mathbf{u} and a supposed photon frequencyable to photo-ionize, a continuity equation can be written. At the second member, the first term expresses the spontaneous emission of n^* , the second term is the absorption

$$c \frac{d\psi_\nu(s)}{ds} = \frac{A_\nu n^*(s)}{4\pi} - \mu c \psi_\nu(s) + n^*(s) c B_\nu \psi_\nu(s)$$

$$c \psi_\nu(s) = \frac{A_\nu}{4\pi} \int_{s_0}^s n^*(s') \exp \left[-\mu c |s' - s| + c B_\nu \int_{s'}^s n^*(s'') ds'' \right] ds'$$

term. The new aspect is the use of the third term, which is the induced de-excitation of n^* by the photon flux. In other words, the streamer is considered as a tiny laser. The distribution function is then in principle given by integration. The objective here is to investigate, if, in such manner, there is a beam directed in the gap axis direction, which increase the photoelectron production near the axis. If this occurs, the electron avalanches extension, at the streamer space charge, should be smaller, and the discharge radius also.

$$\psi_\nu(\vec{r}, \vec{u}) = \frac{1}{4\pi} \varphi_0(\vec{r}) + \frac{3}{4\pi} \varphi_1(\vec{r}) \vec{u}$$

To simplify the process, the angular distribution function is developed in a two term Legendre expansion. It is known as the Eddington approximation. Thus the equation from which φ_0 is obtained is:

$$c\Delta\varphi_0(\vec{r}) - \mu^*(\vec{r})c\vec{\nabla}\varphi_0(\vec{r})\vec{\nabla}\frac{1}{\mu^*(\vec{r})} = 3\mu^{*2}(\vec{r})c\varphi_0(\vec{r}) - 3\mu^*(\vec{r})n^*(\vec{r})A_\nu$$

This equation then can be solved by a solver of the Poisson equation.

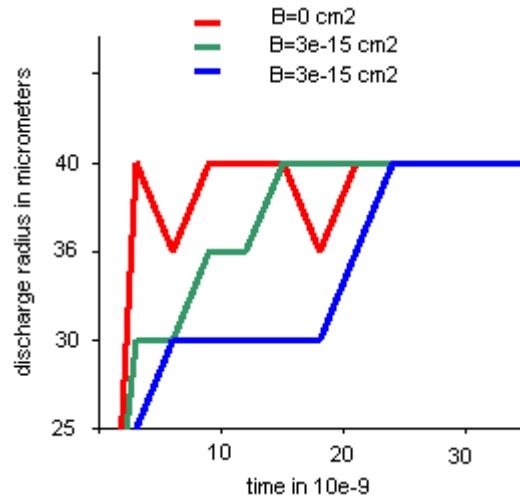


Figure12 Induced emission and discharge radius

These are preliminary results. But, as seen, the induced emission can well induce a lowering of the radial discharge size (fig12). Taking then into account, the electron energy transfer to the neutral, a temperature increase could then be obtained without using a discharge radius taken from the experiment.

4. Conclusions

New applications has fostered the physico-chemical interest in the activities of high pressure streamer discharges. New types of non-thermal plasma reactors, induced by streamer processes, are under consideration. To day, a lot of sets of chemical master equations are presented in view of following the chemical plasma activities. They often apply to homogeneous spatially unbounded case and sometimes only to quasi-stationary case. This presentation was aimed to show that it is not possible to obtain correct physical insights and valuable estimates and figures without taking the spatio-temporal description of hydrodynamic parameters into account.

References

- [¹] Goldman, Corona Discharges, in Gaseous Electronics, N.M.Hirsh, H.J.Oskam, (1978) 1, 219-215
[²]Heuser C., Pietsch G, 1980, 6th Int.Conf.on Gas Dis.and their Applic., Edingburg,IEE Conf.Pub., part1,98-101
[³]J.Amorim, G.Baravian, J.Jolly (2000) J. Phys. D: Appl. Phys. **33** No 9, R51-R65
[⁴] E.Marode,The glow-to-arc transition, in "Electrical Breakdown and Discharges in gases, NATO Series ASI, Serie B volume 89b p. 119-166 (1981).
[⁵]E.Marode, S.Samson , D.Djermoune, N.Deschamps, M.Touzeau, (1999),J.AOT, vol.4 No.1,1999.
[⁶] Advances in Chemical Physics,H Mätzing, LXXX, Ed I Prigogine,John Wiley,315-402 (1991)
[⁷] U.Kogelschatz, Process Technologies for water treatment, S.Stucki, Plenum, 1988
[⁸] F.Bastien, E.Marode, J.Phys.D :Appl.Phys (1979), **12**, 249-263
[⁹]A.A.Kulikovsky, J.Phys D:appl.Phys, (1997)**30**,1515-1522, N.Yu.Babaeva, G.N.Naidis, J.Phys D:appl.Phys, 29 (1996)2423-2431, D.Djermoune, E.Marode, P.Segur (1995)Int.Conf.Phen.Ion.Gas, voll, 33-34
[¹⁰]P.Dessantes, Modeling of streamer type discharges, in air, at high pressure, (2000), Thesis, Orsay University, France